Quantum phase transition and criticality in quasi-one-dimensional spinless Dirac fermions

Yasuhiro Tada [*]
Institute for Solid State Physics, University of Tokyo, Kashiwa 277-8581, Japan

(Received 1 July 2019; revised manuscript received 30 August 2019; published 20 September 2019)

We study the quantum criticality of spinless fermions on a quasi-one-dimensional π-flux square lattice in cylinder geometry, by using the infinite density matrix renormalization group and Abelian bosonization. For a series of cylinder circumferences $L_y = 4n + 2 = 2, 6, \ldots$ with a periodic boundary condition, there are quantum phase transitions from gapped Dirac fermion states to charge density wave (CDW) states. We find that the quantum phase transitions for such circumferences are continuous and belong to the (1+1)-dimensional Ising universality class. On the other hand, when $L_y = 4n = 4, 8, \ldots$, there are gapless Dirac fermions at the noninteracting point and the phase transition to the CDW state is Gaussian. Both of these criticalities are described in a unified way by bosonization. We clarify their intimate relationship and demonstrate that a central charge $c = 1/2$ Ising transition line arises as a critical state of an emergent Majorana fermion from the $c = 2$ Gaussian transition point.

DOI: 10.1103/PhysRevB.100.125145

I. INTRODUCTION

Criticality associated with a phase transition is one of the central issues in condensed matter physics. Various phase transitions have been established mainly for insulators which are well described by bosonic models such as Ising, XY, and Heisenberg models. However, phase transitions in *metals* where gapless fermions are coupled with bosons are rather poorly understood compared to insulators only with bosons. In such a system, fermions strongly affect the low-energy behaviors of the bosonic order parameters and consequently could change the criticality of the phase transition. The critical bosonic fluctuations in turn influence the fermions, and the resulting non-Fermi-liquid-like behaviors are often observed in various systems [1–4].

The criticality depends on the structures of fermionic excitations such as the dimensionality of the Fermi surface and the number of fermion flavors (orbitals and spins). One of the simplest examples is spinless fermions on a one-dimensional (1D) chain at half filling with the nearest-neighbor repulsive interaction V, where the classical ground states for $V \to \infty$ are the charge density wave (CDW) states [5,6]. When one introduces fermionic hopping t, there will be a Kosterlitz-Thouless phase transition to a Tomonaga-Luttinger liquid, which is distinct from the Ising transition in bosonic models. Quantum criticalities in higher-dimensional systems are also of great interest, and in this context, a semimetallic system is an ideal platform to study the interplay between fermions and bosons where the Fermi surface is a point. Indeed, the critical behaviors of phase transitions in Dirac systems have been extensively studied, and gapless Dirac excitations can lead to new criticalities such as chiral Ising, chiral XY, and chiral Heisenberg universality classes [7–22]. The critical exponents of these phase transitions have been evaluated accurately by several methods, e.g., analytical calculations and unbiased quantum Monte Carlo simulations. In these (semi)metallic systems, the gapless fermions play essential roles and the resulting quantum criticality is different from that in a corresponding purely bosonic system with gapped fermions.

These two criticalities are usually studied separately as distinct properties of metals and insulators. For example, the quantum phase transition from a gapless Dirac state to an antiferromagnetic state in a honeycomb lattice is described by the (2+1)D chiral Heisenberg universality class, while the one from a spin-orbit coupled gapped Dirac state to the antiferromagnetic state belongs to the 3D XY universality class [13,23,24]. Similarly, one can separately discuss the two criticalities of the phase transitions from a metal or a band insulator to an ordered state in general. However, such separate discussions would be somewhat subtle when the band gap is very small, and there will be a crossover between fermionic criticality and bosonic criticality in a narrow gap system. Then, a natural question is how these two criticalities are connected along the critical line of the phase transition in an extended phase diagram including both metals and insulators (Fig. 1). Experimentally, Dirac fermions can be found not only in bulk materials but also in cold atoms [25,26]. Especially in the latter systems, a Dirac band gap could be tuned by changing the system geometry, and distinct critical behaviors might be potentially observed.

In this paper, we consider quasi-1D half-filled spinless fermions on a π-flux square lattice in cylinder geometry with the circumference L_y, as a simple example of the quantum phase transition of $\mathbb{Z}_2$ symmetry breaking. When the nearest-neighbor repulsive interaction V is weak, there are Dirac fermions with a mass m due to the finite system size L_y for $L_y = 2, 6, 10, \ldots$ under the periodic boundary condition

[*]tada@issp.u-tokyo.ac.jp

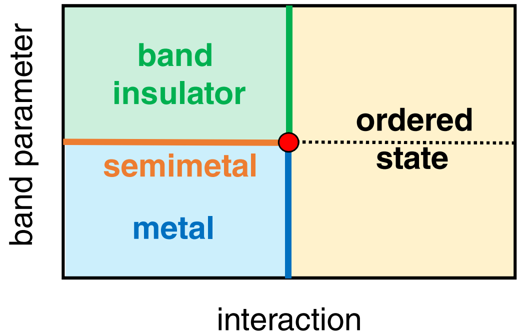

FIG. 1. A schematic phase diagram including both insulating and (semi)metallic states. Generally, the blue and green phase transition lines and the red transition point would be characterized by different criticalities.

along the y direction, while there are gapless Dirac fermions at $V = 0$ for $L_y = 4n = 4, 8, \ldots$. The system exhibits a staggered CDW ordered state for large V. The quantum phase transition is studied with use of the infinite density matrix renormalization group (iDMRG) [27–32] together with the recently developed scaling analysis [16]. Then, we demonstrate that the quantum phase transition at a critical $V = V_c > 0$ between the gapped Dirac fermions and the CDW state is continuous, and the corresponding criticality is simply a (1+1)D Ising universality class. On the other hand, the iDMRG results suggest that the phase transition from the gapless Dirac state is smooth around $V = 0$, which turns out to be Gaussian. These two behaviors are well described within the bosonization approach in a unified manner, and a global phase diagram in the V-m plane is discussed. We clarify their intimate relationship and demonstrate that the central charge $c = 1/2$ Ising transition line arises as a critical state of an emergent Majorana fermion from the $c = 2$ Gaussian transition point.

II. MODEL AND PHASE TRANSITION

A. Model

We consider spinless fermions on a π-flux square lattice at half filling,

$$H = -\sum_{\langle i,j\rangle} t_{ij} c_i^\dagger c_j + V \sum_{\langle i,j\rangle} n_i n_j, \tag{1}$$

where $t_{ij} = t(-t)$ along the x direction at even (odd) y_i and $t_{ij} = t$ along the y direction. $\langle i, j\rangle$ represents a pair of nearest-neighbor sites (Fig. 2). We use the energy unit $t = 1$. The system size is $L_x \times L_y = \infty \times L_y$ with the periodic boundary condition for the y direction otherwise specified. We consider only even L_y's in the present study, because the CDW order is staggered. In 2D ($L_y = \infty$) at $V = 0$, this model has two Dirac points and there is a continuous quantum phase transition to a staggered CDW state at $V_c \simeq 1.30t$ [9–12]. The criticality of the CDW phase transition belongs to the (2+1)D chiral Ising universality class, whose critical exponents are evaluated as $\beta \simeq 0.60 \pm 0.07$ and $\nu \simeq 0.79$–0.80 by the quantum Monte Carlo calculations [9–12].

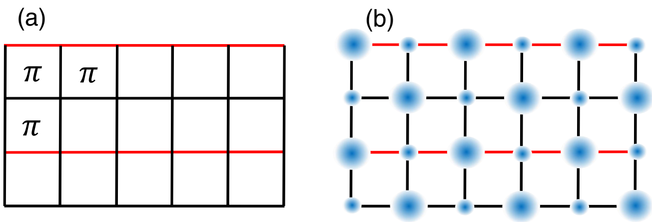

FIG. 2. (a) An $L_y = 4$ π-flux square lattice with the periodic boundary condition. The hopping on the black bonds is $-t$ and that on the red bonds is $+t$, which gives a π flux for each square plaquette. (b) Schematic picture of the staggered CDW order. The blue circles represent the fermion particle density.

For a finite $L_y > 2$, the single-particle dispersion under the periodic boundary condition for the y direction is given by

$$\varepsilon(k_x, k_y) = \pm\sqrt{(2t\cos k_x)^2 + (2t\cos k_y)^2}, \tag{2}$$

where k_x takes continuum values and $k_y = 2\pi n/L_y$ ($n = 0, 1, \ldots, L_y/2 - 1$). Similarly, $\varepsilon(k_x) = \pm\sqrt{(2t\cos k_x)^2 + t^2}$ for $L_y = 2$. Due to the discreteness of k_y, the dispersion is qualitatively different when $L_y = 4n = 4, 8, 12, \ldots$ and $L_y = 4n + 2 = 2, 6, 10, \ldots$; the gapless Dirac points exist for $L_y = 4n$, while the Dirac fermions are massive with the gap size $m \sim t/L_y$ for $L_y = 4n + 2$. $\varepsilon(k)$ is shown in Fig. 3 for $L_y = 8$ and $L_y = 10$ as an example. Note that if the antiperiodic boundary condition is imposed for the y direction, systems with $L_y = 4n + 2$ become massless while those with $L_y = 4n$ are massive. This property will be used later in Sec. II C.

To discuss the effects of the interaction V, we use iDMRG for a system of cylinder geometry and Abelian bosonization. The iDMRG allows a highly accurate calculation, and has been used extensively not only for one-dimensional systems but also for two-dimensional systems. One can directly describe a quantum phase transition of discrete symmetry in such an infinite length cylinder by using iDMRG. Later, we also perform a bosonization analysis around $V = 0$ but with a twisted boundary condition for the y direction, which enables us to discuss the gapped and gapless fermions on equal footing.

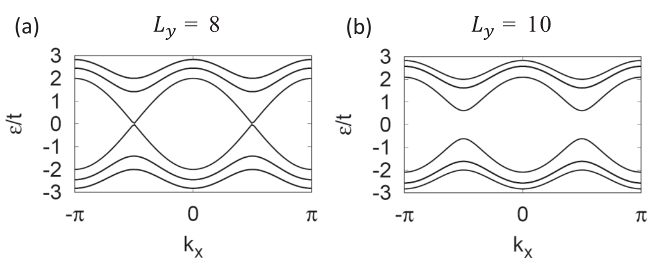

FIG. 3. Single-particle dispersion relations (a) for $L_y = 8$ and (b) for $L_y = 10$ under the periodic boundary condition in the y direction.

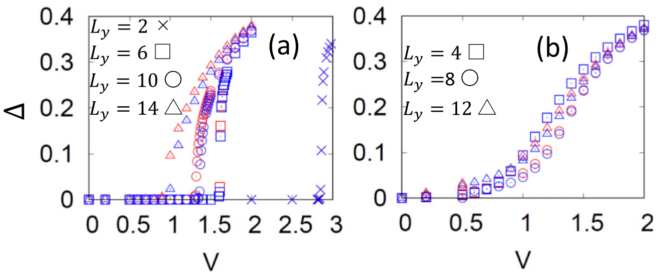

FIG. 4. The CDW order parameter Δ as a function of the interaction V calculated by iDMRG with the periodic boundary condition for the y direction. (a) $L_y = 4n + 2 = 6, 10, 14$ with $\chi = 1000$ (red), 1600 (blue). For $L_y = 2$, $\chi = 100$ (red), 200 (blue). (b) $L_y = 4n = 4, 8, 12$ with $\chi = 1000$ (red), 1600 (blue). Note that the data for $L_y = 2, 4$ with the different values of χ almost coincide in the present scale of the figures.

B. iDMRG calculations

1. Order parameter

In this section, the CDW quantum phase transition is investigated by iDMRG [27–30] with use of the open source code TeNPy [31,32]. In this study, we consider different system sizes $L_y = 2$–14 with $L_x = \infty$, and the discarded weights by the truncation in iDMRG calculations are typically of order 10^{-10}, 10^{-8}, 10^{-8}, 10^{-6}, 10^{-5}, 10^{-5}, and 10^{-4} for $L_y = 2$, 4, 6, 8, 10, 12, and 14, respectively, when the largest bond dimensions are used. First of all, we discuss the CDW order parameter associated with the $\mathbb{Z}_2$ symmetry breaking,

$$\Delta = \frac{1}{L'_x L_y} \sum_i (-1)^{|i|} n_i, \tag{3}$$

where L'_x is the unit period assumed in the iDMRG calculation. The summation is over $x = 1, 2, \dots, L'_x$ and $y = 1, 2, \dots, L_y$. We have performed calculations for various L'_x and confirmed that the results are essentially independent of L'_x. First, we show $|\Delta|$ for the massive case ($L_y = 4n + 2$) and massless case ($L_y = 4n$), respectively, in Fig. 4. For the massive case $L_y = 2, 6, 10, 14$, we find a clear quantum phase transition from the gapped Dirac state to the CDW state at L_y-dependent critical values $V = V_c(L_y) > 0$. The critical value $V_c(L_y)$ decreases as L_y increases for a fixed bond dimension χ, because the Dirac band mass $m \sim t/L_y$ is reduced for larger L_y. We expect that $V_c(L_y)$ is monotonically decreasing and approaches the 2D value $V_c(\infty) = 1.30$, because a band gap will usually suppress the effects of interactions. Indeed, $V_c(L_y = 14)$ is larger than $V_c(\infty) = 1.30$ since an extrapolated value of $\Delta(L_y = 14, V = 1.3)$ to $\chi = \infty$ is zero. On the other hand, for the massless case with $L_y = 4, 8, 12$, the order parameter Δ behaves smoothly as a function of V, where the gapless Dirac states can be correctly described only when the bond dimension χ in the iDMRG calculation is infinitely large, $\chi \to \infty$. In this limit, we expect a Gaussian transition takes place at $V = 0$, which is indeed described by the bosonization in the latter section. In the next part, we focus on the massive case $L_y = 4n + 2$ and discuss its criticality within iDMRG.

2. Finite correlation length scaling for $L_y = 4n + 2$

The criticality of the phase transition for $L_y = 4n + 2 = 2, 6, 10, \dots$ is expected to be of the (1+1)D Ising universality class if it is continuous, because the CDW state breaks $\mathbb{Z}_2$ translation symmetry and there is no gapless Dirac fermions at $V = 0$ for these L_y. In order to examine the criticality and confirm this expectation numerically, we use the scaling ansatz recently developed for tensor network states in an infinite projected entangled pair state (iPEPS) [16]. Since the one-dimensional system size L_x is infinite in iDMRG, finite-size effects of the criticality are controlled not by $L_x = \infty$ but by the correlation length ξ_χ in our calculations. The correlation length ξ_χ is computed from the second largest eigenvalue of the transfer matrix for a given bond dimension χ, and ξ_χ characterizes finite bond dimension effects. One would naively expect that the system may exhibit (2+1)D chiral Ising criticality if $\xi_\chi \ll L_y$, while it shows (1+1)D bosonic Ising criticality if $\xi_\chi \gg L_y$. In the following, we focus only on the latter case with $\xi_\chi \gg L_y$.

The scaling ansatz for the ground-state energy density is written as

$$E\left(g, h, \xi_\chi^{-1}\right) = b^{-2} E\left(b^{y_g} g, b^{y_h} h, b\xi_\chi^{-1}\right), \tag{4}$$

where $g = [V - V_c(L_y)]/V_c(L_y)$ and h is the conjugate field to Δ with the corresponding scaling dimensions y_g and y_h. We have assumed the dynamical critical exponent is $z = 1$. The correlation length ξ_χ determined by the bond dimension χ characterizes finite-size effects in the present $L_x = \infty$ system [16]. This finite correlation length scaling ansatz takes the same form as the conventional finite-size scaling ansatz often used in a Monte Carlo calculation for a system of size L, $E(g, h, L^{-1}) = b^{-2} E(b^{y_g} g, b^{y_h} h, bL^{-1})$. The L_y-dependent critical points $V_c(L_y)$ are determined so that a scaling behavior of the order parameters Eqs. (7) and (8) holds for larger ξ_χ. We obtain $V_c(L_y = 2) \simeq 2.8678$, $V_c(6) \simeq 1.624$, and $V_c(10) \simeq 1.5$ as will be discussed in the following. Near the critical point, the order parameter and correlation length ξ at $\chi = \infty$ behaves as

$$\Delta(g) \sim g^\beta \quad (g \geqslant 0), \tag{5}$$

$$\xi(g) \sim |g|^{-\nu}. \tag{6}$$

On the other hand, at the critical point $g = 0$, the CDW order parameter for finite χ exhibits the scaling behaviors

$$\Delta(g = 0) \sim \xi_\chi^{-\beta/\nu}, \tag{7}$$

$$\frac{\partial_g \Delta(g = 0)}{\Delta(0)} \sim \xi_\chi^{1/\nu}, \tag{8}$$

which are derived from the scaling ansatz Eq. (4) similarly to the conventional finite-size scaling [16]. From these two equations, we can determine the critical exponents β and ν. Table I summarizes the iDMRG results. The critical interaction $V_c(L_y)$ and critical exponents are estimated from the scaling relations (7) and (8), and the central charge c from the entanglement entropy Eq. (10). These results clearly suggest that the phase transition from the gapped Dirac insulator to the CDW state indeed belongs to the Ising universality class, as we have expected. It is noted that we have used only

TABLE I. Summary of the iDMRG results. The corresponding values for the (1+1)D Ising universality class are also listed for comparison.

	Ising_{1+1}	$L_y = 2$	$L_y = 6$	$L_y = 10$
V_c		2.8678	1.624	1.5
β/ν	1/8	0.128(1)	0.123(1)	0.150(2)
$1/\nu$	1	1.02(1)	1.07(1)	0.94(4)
c	1/2	0.510(3)	0.502(1)	

the numerical data with $\xi_\chi > L_y$, but the correlation length for $L_y = 10$ is at most $\xi_\chi \sim 20$ even with the largest χ and therefore the scaling analysis is not so reliable for this system size. Especially, the calculated entanglement entropy for $L_y = 10$ is not well fitted by the scaling behavior [Eq. (10)], because of the short correlation length for χ used in the calculation. In the following, we discuss the scaling analysis in more detail.

In Fig. 5, we show the ξ_χ dependence of Δ and $\partial_g\Delta/\Delta$ for $L_y = 2$, where the different ξ_χ corresponds to different bond dimensions χ. Equation (7) is approximated as $\partial_g\Delta/\Delta = \{V[\Delta(V+\delta V) - \Delta(V-\delta V)]/2\delta V\}/\{[\Delta(V+\delta V) + \Delta(V-\delta V)]/2\}$ with $\delta V = 0.0001$, and we have confirmed convergence of the results by using different δV. First of all, the quantum phase transition is continuous since the scaling behaviors hold up to large $\xi_\chi > 1000$, although a discontinuous transition was potentially possible. The critical interaction strength is obtained as $V_c(L_y = 2) = 2.8678$ from the figure, where the scaling behaviors hold in the widest region of ξ_χ. When the system goes away from the critical point, Δ starts to deviate from the scaling behaviors at a length scale set by the interaction. The critical behaviors of Δ are in good agreement with those of the (1+1)D Ising universality class with $\beta = 0.125$, $\nu = 1$, as we have expected. Similarly, we show the ξ_χ dependence of Δ and $\partial_g\Delta/\Delta$ for $L_y = 6$ in Fig. 6, where $\partial_g\Delta/\Delta$ is approximated in the same way as in the $L_y = 2$ case. The critical interaction is evaluated as $V_c(L_y = 6) = 1.624$, where the scaling behaviors are satisfied up to $\xi_\chi \sim 100$–1000. Although there is some signature for a dimensional crossover from the (2+1)D chiral Ising universality class for small $\xi_\chi \lesssim L_y$, the true criticality close to the critical point $g = 0$ belongs to the (1+1)D Ising universality class. For $L_y = 10$, however, it is difficult to explicitly demonstrate the critical behavior of the (1+1)D Ising universality class as shown in Fig. 7, because of the heavy finite χ effects. Here, we used χ up to 2400, and the critical interaction is roughly estimated to be $V_c(L_y = 10) \simeq 1.5$. We think that the critical behavior of the (1+1)D Ising universality class will be reproduced for sufficiently large χ similarly to the cases for $L_y = 2, 6$.

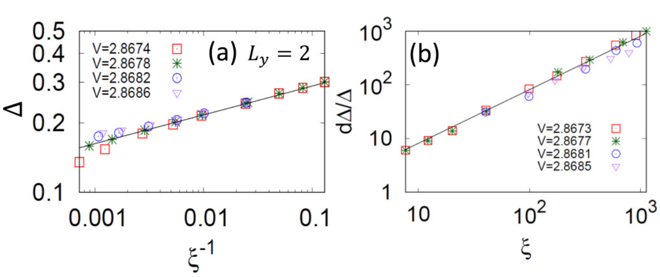

FIG. 5. The scaling plots of the CDW order parameter for $L_y = 2$. The correlation length ξ_χ is denoted as ξ for simplicity. (a) The scaling plot Eq. (7), and the black line is $\Delta \sim \xi^{-\beta/\nu}$ with $\beta = 0.125$, $\nu = 1$. (b) The scaling plot Eq. (8), and the black line is $\partial_g\Delta/\Delta \sim \xi^{1/\nu}$ with $\nu = 1$. The g derivative is approximated by $\partial_g\Delta(V) = V_c[\Delta(V+\delta V) - \Delta(V-\delta V)]/2\delta V$ with $\delta V = 0.0001$. The bond dimension is used up to $\chi \leqslant 200$.

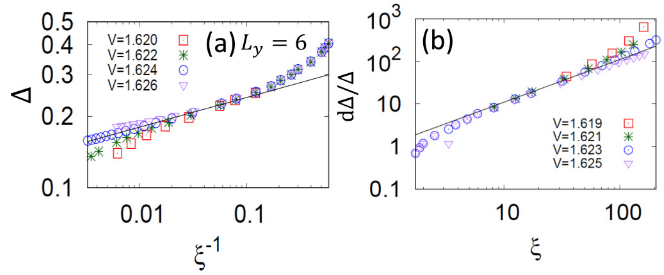

FIG. 6. The scaling plots of the CDW order parameter for $L_y = 6$. (a) The scaling plot Eq. (7) and (b) Eq. (8). The black lines are the same as in Fig. 5, while the g derivative is approximated with $\delta V = 0.001$. The bond dimension is used up to $\chi \leqslant 2800$.

To further confirm the critical behaviors of the (1+1)D Ising universality class, in Fig. 8, we show the scaling plot

$$\Delta\xi_\chi^{\beta/\nu} = \mathcal{M}\big(g\xi_\chi^{1/\nu}\big), \tag{9}$$

where $\mathcal{M}$ is a scaling function [16]. It is noted that this scaling behavior takes the same form as the conventional one for a finite-size system, $\Delta L^{\beta/\nu} = \tilde{\mathcal{M}}(gL^{1/\nu})$. Here, we have used only the data for $\xi_\chi > L_y$ to avoid the effects of the dimensional crossover, and simply employed the critical exponents of the (1+1)D Ising universality class $\beta = 1/8$, $\nu = 1$ with the critical interactions obtained above $V_c(L_y = 2) = 2.8678$, $V_c(6) = 1.624$. Clearly, all the data collapse into a single curve in each system size $L_y = 2, 6$, which gives a cross-check for the Ising universality class of the CDW phase transition.

Finally, we discuss the central charge c of the effective field theory for the criticality. Figure 9 shows the entanglement entropy S for bipartitioning the infinite one-dimensional chain in the iDMRG calculation into two half-infinite chains. In such bipartitioning, the entanglement entropy at the critical point is characterized by the central charge c of the underlying

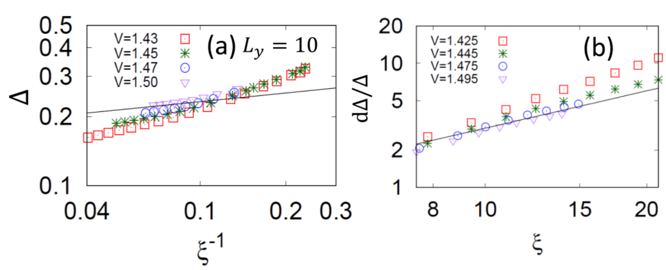

FIG. 7. The scaling plots of the CDW order parameter for $L_y = 10$. (a) The scaling plot Eq. (7) and (b) Eq. (8). The black lines are the same as in Fig. 5, while the g derivative is approximated with $\delta V = 0.005$. The bond dimension is used up to $\chi \leqslant 2400$.

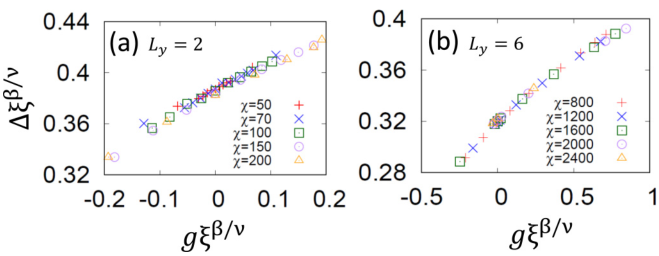

FIG. 8. The scaling plot of the CDW order parameter Δ for (a) $L_y = 2$ and (b) $L_y = 6$. The critical exponents used are those for the (1+1)D Ising universality class $\beta = 0.125$, $\nu = 1$.

conformal field theory and is given by

$$S = \frac{c}{6} \ln \xi_\chi + S_0, \tag{10}$$

where S_0 is a constant [31,33]. In the present system, the calculated S at the critical point is well fitted by this formula with $c = 1/2$, which means that the corresponding conformal field theory is the $c = 1/2$ Ising theory in agreement with the critical behaviors of the order parameter Δ.

In this section, we have discussed the CDW order parameter and did not directly examine the corresponding energy gap. It is noted that when $L_y = 4n + 2$, the single-particle excitation gap remains nonzero for all V through the phase transition as seen in the previous study for a related model [24] and the bosonization analysis of the present model in the next section. On the other hand, the collective charge excitation gap vanishes at the transition point with a power-law behavior. The charge gap should show a universal behavior corresponding to the Ising universality class, and therefore the gap will be $\sim\xi^{-1} \sim |g|^\nu$ with $\nu = 1$, which can be explicitly shown in the conventional transverse Ising model.

C. Bosonization and global phase diagram

In this section, we discuss the relationship between the CDW phase transitions from gapless and gapped Dirac states within the bosonization approach [5,6,34,35]. Our primary purpose is to find an effective theory description for the iDMRG calculation results. To discuss the gapless and gapped states on equal footing, it is convenient to treat the band gap as a continuous parameter rather than a discrete parameter characterized only by L_y as $m \sim t/L_y$. So, we introduce the twisted boundary condition with the twist angle θ for the

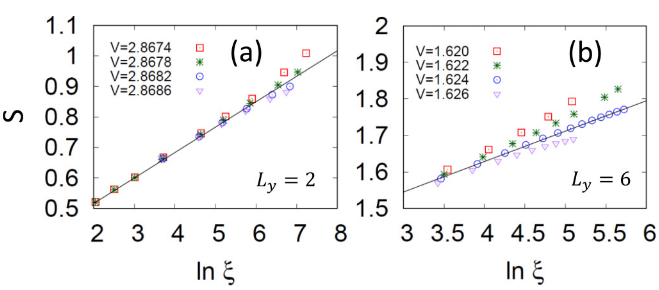

FIG. 9. The entanglement entropy S for (a) $L_y = 2$ and (b) $L_y = 6$. The black lines are $S = (c/6)\ln\xi + S_0$ with the central charge $c = 1/2$.

y direction, or equivalently insert a flux θ along the cylinder with the vector potential $A_{i,i+\hat{y}} = \theta/L_y$ [36]. When $\theta = 0$, the periodic boundary condition is realized and the noninteracting Dirac fermions are gapless for $L_y = 4n$. The band gap in Eq. (2) is continuously tuned by the twisting angle θ since the allowed discrete k_y [$=(2\pi n + \theta)/L_y$] points for given finite L_y changes as θ is varied. For example, in the $L_y = 4n$ case, the band gap becomes maximum at $\theta = \pi$, for which there is a CDW phase transition from a gapped Dirac state whose criticality is the (1+1)D Ising universality class. In this way, one can smoothly connect the two extreme cases, the gapless Dirac semimetal and maximally gapped Dirac band insulator for a fixed system size L_y, while changing L_y for a fixed θ can tune the Dirac band mass only discretely.

We consider the noninteracting excitation spectra in the π-flux cylinder with a fixed $L_y = 4n$ under the periodic boundary condition as shown in Fig. 3(a), and focus only on the gapless Dirac fermion branches and neglect other gapped bands. (A system with $L_y = 4n + 2$ can be discussed in a similar way.) There are two pairs of linear dispersions with positive and negative velocities around $k_x = \pm\pi/2$. If we introduce a twist angle $0 \leqslant \theta \leqslant 2\pi$, a band gap $m(\theta)$ will be induced in the preexisting gapless Dirac bands. The two branches can be reproduced by an effective two-leg ladder model,

$$\begin{aligned} H_{\text{eff}} = &\sum_{s=1,2} \sum_i -t_s c_{is}^\dagger c_{i+1s} - t_\perp \sum_i c_{i1}^\dagger c_{i2} + (\text{H.c.}) \\ &+ \tilde{U} \sum_i n_{i1} n_{i2} + \tilde{V} \sum_{s=1,2} \sum_i n_{is} n_{i+1s}, \end{aligned} \tag{11}$$

where $t_s = (-1)^{s+1} t$, $t_\perp = 2t|\cos(\pi/2 + \theta/L_y)|$, $\tilde{U} = 2V/L_y$, $\tilde{V} = V/L_y$ for a fixed $L_y = 4n$. [In the case of a fixed $L_y = 4n + 2$, the interchain hopping is $t_\perp = 2t|\cos(\pi/2 + \theta/L_y - \pi/L_y)|$.] It is easy to see that this effective model indeed reproduces the low-energy spectra of the original model Eq. (1) at $V = 0$, and also correctly describes the interaction within this low-energy subspace. A similar effective model was studied before in the context of carbon nanotubes [34]. By using the transformation $c_{i1} \to c_{i1}$, $c_{i2} \to (-1)^i c_{i2}$, the Hamiltonian is rewritten into the familiar form with an additional staggered hybridization term $(-1)^i t_\perp$,

$$\begin{aligned} H_{\text{eff}} \to &\sum_{s=1,2} \sum_i -t c_{is}^\dagger c_{i+1s} - t_\perp \sum_i (-1)^i c_{i1}^\dagger c_{i2} + (\text{H.c.}) \\ &+ \tilde{U} \sum_i n_{i1} n_{i2} + \tilde{V} \sum_{s=1,2} \sum_i n_{is} n_{i+1s}, \end{aligned} \tag{12}$$

where hopping along the chain is t for both $s = 1, 2$.

The fermion operators are approximated around the Fermi point $k_F = \pm\pi/2a$ as $\psi_s(x) = e^{-ik_F x}\psi_{Ls}(x) + e^{ik_F x}\psi_{Rs}(x)$ with $\psi_{rs}(x) = \eta_{rs} e^{-i(r\phi_s - \theta_s)}/\sqrt{2\pi a}$, where a is the lattice constant and η_{rs} is the Klein factor [5,6]. The bosonic phase operators satisfy the commutation relation

$$[\phi_s(x), \partial_{x'}\theta_{s'}(x')] = i\pi\delta_{ss'}\delta(x - x'). \tag{13}$$

Furthermore, we introduce new fields $\phi_{0,\pi} = (\phi_1 \pm \phi_2)/\sqrt{2}$ for convenience. Then the Hamiltonian is bosonized into

$$\begin{aligned}H_{\rm eff} &= H_{\rm kin} + H_{\rm int},\\ H_{\rm kin} &= \sum_{k=0,\pi} \frac{v_k}{2\pi}\int dx[K_k^{-1}(\partial\phi_k)^2 + K_k(\partial\theta_k)^2],\\ H_{\rm int} &= \int dx\Big[g_1\cos\sqrt{8}\phi_0 + g_2\cos\sqrt{8}\phi_\pi\\ &\quad + g_3\cos\sqrt{8}\phi_0\cos\sqrt{8}\phi_\pi + g_4\cos\sqrt{2}\phi_0\sin\sqrt{2}\theta_\pi\Big],\end{aligned} \tag{14}$$

where $g_1 = -\tilde{U}/2\pi^2 a$, $g_2 = \tilde{U}/2\pi^2 a$, $g_3 = \tilde{V}/\pi^2 a$, $g_4 = 2t_\perp/\pi a$. For small $\tilde{U}, \tilde{V}$, the parameters are given by $v_0 = v_F/K_0$, $v_\pi = v_F/K_\pi$, and

$$K_0^{-1} = \sqrt{1 + \frac{a}{\pi v_F}(\tilde{U} + 4\tilde{V})} \simeq 1 + \frac{a}{2\pi v_F}(\tilde{U} + 4\tilde{V}), \tag{15a}$$

$$K_\pi^{-1} = \sqrt{1 + \frac{a}{\pi v_F}(-\tilde{U} + 4\tilde{V})} \simeq 1 + \frac{a}{2\pi v_F}(-\tilde{U} + 4\tilde{V}), \tag{15b}$$

where $v_F = 2t$ is the Fermi velocity of the noninteracting model. The scaling dimensions of the operators are easily read off as

$$[g_1] = 2K_0 \simeq 2 - \frac{a}{\pi v_F}(\tilde{U} + 4\tilde{V}), \tag{16a}$$

$$[g_2] = 2K_\pi \simeq 2 - \frac{a}{\pi v_F}(-\tilde{U} + 4\tilde{V}), \tag{16b}$$

$$[g_3] = 2K_0 + 2K_\pi \simeq 4 - \frac{8a}{\pi v_F}\tilde{V}, \tag{16c}$$

$$[g_4] = \frac{K_0}{2} + \frac{1}{2K_\pi} \simeq 1 - \frac{a}{2\pi v_F}\tilde{U}. \tag{16d}$$

We first consider the case with $t_\perp = 0$, or equivalently $g_4 = 0$. Then, the most relevant term is the g_1 term, and the ϕ_0 field gets pinned to $\langle\phi_0\rangle = 0$ because of the strong coupling $g_1 \to -\infty$. The remaining g_2, g_3 terms will have the same functional form, $\cos\sqrt{8}\phi_\pi$, and be renormalized to $g_2, g_3 \to \infty$. Therefore, both of the fields ϕ_0, ϕ_π become gapped as long as $V > 0$, and the phase transition is a Gaussian transition from the $c = 2$ two-flavor gapless Dirac state to the fully gapped CDW state. This is consistent with the iDMRG calculation where the CDW order parameter is nonzero for very small V when $L_y = 4n = 4, 8, \ldots$ under the periodic boundary condition.

Next, we consider a very small $0 < t_\perp \ll V$, for which the renormalized parameters still satisfy $|g_4| \ll |g_1|$ down to some energy scale under the renormalization group. In this energy scale, the ϕ_0 field is nearly locked as $\langle\phi_0\rangle \simeq 0$ and the low-energy physics is described by the ϕ_π field only,

$$\begin{aligned}H_{\rm eff} \simeq& \frac{v_\pi}{2\pi}\int dx\big[K_\pi^{-1}(\partial\phi_\pi)^2 + K_\pi(\partial\theta_\pi)^2\big]\\ &+ \int dx\Big[g_{23}\cos\sqrt{8}\phi_\pi + g_4\sin\sqrt{2}\theta_\pi\Big],\end{aligned} \tag{17}$$

where $g_{23} = g_2 + g_3$ and we have used the approximation $\langle\cos\sqrt{8}\phi_0\rangle \simeq \langle\cos\sqrt{2}\phi_0\rangle \simeq 1$. Note that the parameters in Eq. (17) should be regarded as renormalized ones under the renormalization group flow down to the above-mentioned energy scale. In this Hamiltonian, the g_{23} term favors the CDW state while the g_4 term leads to the band insulator, and this competition can lead to a gapless state when these two perturbations cancel each other. The resulting gapless state is described by the $c = 1/2$ Majorana fermions, which corresponds to the criticality of the CDW phase transition from the band gapped Dirac state discussed in the previous section. To see this, we focus on a fine-tuned state where the two perturbation terms are maximally competing having the same scaling dimensions, $[g_{23}] = [g_4]$, namely,

$$2K_\pi = \frac{1}{2K_\pi} \Rightarrow K_\pi = \frac{1}{2}. \tag{18}$$

By redefining the boson fields as $\phi'_\pi = \phi_\pi/\sqrt{K_\pi}$, $\theta'_\pi = \sqrt{K_\pi}\theta_\pi - \pi/4$ with $K_\pi = 1/2$, the Hamiltonian is rewritten as

$$\begin{aligned}H_{\rm eff} =& \frac{v_\pi}{2\pi}\int dx\Big[\big(\partial\phi'_\pi\big)^2 + \big(\partial\theta'_\pi\big)^2\Big]\\ &+ \int dx\big[g_{23}\cos 2\phi'_\pi + g_4\cos 2\theta'_\pi\big].\end{aligned} \tag{19}$$

This Hamiltonian is called the self-dual sine-Gordon model and has been studied extensively [6,37–40]. Since the scaling dimensions of both g_{23}, g_4 terms are 1, one can refermionize them by using a spinless fermion operator $\psi_r(x) \simeq \eta_r e^{-i(r\phi'_\pi - \theta'_\pi)}/\sqrt{2\pi a}$ as

$$\cos 2\phi'_\pi = -i\pi a\big[\psi_R^\dagger\psi_L - \psi_L^\dagger\psi_R\big], \tag{20a}$$

$$\cos 2\theta'_\pi = -i\pi a\big[\psi_R^\dagger\psi_L^\dagger - \psi_L\psi_R\big]. \tag{20b}$$

Therefore the self-dual sine-Gordon model is mapped to a free spinless fermion model with mass terms,

$$\begin{aligned}H_{\rm eff} =& \int dx - iv_\pi[\psi_R^\dagger\partial\psi_R - \psi_L^\dagger\partial\psi_L]\\ &- im_{23}[\psi_R^\dagger\psi_L - \psi_L^\dagger\psi_R] - im_4[\psi_R^\dagger\psi_L^\dagger - \psi_L\psi_R],\end{aligned} \tag{21}$$

where $m_{23} = \pi a g_{23}$, $m_4 = \pi a g_4$ Then we introduce Majorana fermions $\gamma^1 = (\psi + \psi^\dagger)/\sqrt{2}$, $\gamma^2 = (\psi - \psi^\dagger)/\sqrt{2}i$ to write the Hamiltonian in the Majorana basis,

$$H_{\rm eff} = \sum_{a=1,2}\int dx - i\frac{v_\pi}{2}\big[\gamma_R^a\partial\gamma_R^a - \gamma_L^a\partial\gamma_L^a\big] - im_{\gamma a}\gamma_R^a\gamma_L^a, \tag{22}$$

where $m_{\gamma 1} = m_{23} + m_4$, $m_{\gamma 2} = m_{23} - m_4$. Clearly, only one Majorana fermion γ_2 is gapless and the other one γ_1 is gapped along the special line given by $m_{23} = m_4$ in the V-$t_\perp$ plane. (Note that we have assumed $t_\perp > 0$ and thus $m_{\gamma 1} \neq 0$ in this study.) This emergent gapless Majorana fermions describe the $c = 1/2$ conformal field theory which is the critical theory for the CDW phase transition from the band gapped Dirac state studied in the previous section. Physically, the Majorana fermions correspond to domain walls of the CDW oder. Finally, it is noted that the fermion single-particle gap stays nonzero at the Ising critical point since the ϕ_0-boson field

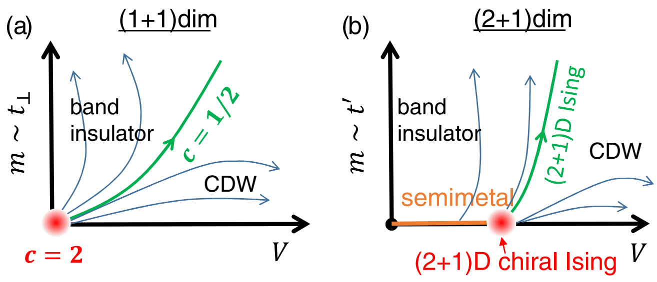

FIG. 10. (a) Schematic global phase diagram in the V-$t_\perp$ plane in (1+1)D. The red point at the origin is the $c = 2$ Gaussian transition point, and the green curve is the $c = 1/2$ Ising transition line separating the band insulator and CDW state. The arrows correspond to the renormalization group flow in the effective low-energy model. (b) Expected phase diagram in (2+1)D. t' is an additional hopping which induces a band gap.

which is a part of the fermion is gapped [5,6], as pointed out in the last paragraph of Sec. II B 2.

We have shown within the bosonization how the fermionic criticality at the Gaussian transition is connected to the bosonic criticality at the Ising transition. These discussions are summarized in the global phase diagram shown in Fig. 10. For example, a Dirac band insulator with a mass $m \sim t/L_y$ is realized for small V in a system with $L_y = 4n + 2(4n)$ with the periodic (antiperiodic) boundary condition, while the system is gapless at $V = 0$ in a system with $L_y = 4n + 2(4n)$ with the antiperiodic (periodic) boundary condition. Correspondingly, the band insulator exhibits the Ising phase transition to a CDW state, while the semimetal shows the CDW order for all $V > 0$. These behaviors are consistent with the iDMRG results in the previous section. We expect that competition between the band gap and interaction would be important also for higher dimensions. For example, in spinless fermions on the two-dimensional π-flux square lattice, there is a CDW quantum phase transition with (2+1)D chiral Ising criticality at $V = V_c > 0$ from the gapless Dirac semimetal [9–12], while a transition from the gapped Dirac insulator is expected to show 3D Ising criticality if it is continuous. The two phase transitions would be connected in a nontrivial way, and the familiar 3D Ising criticality might be understood as a critical state of an emergent object from the (2+1)D chiral Ising critical point. Further studies are necessary to develop a theoretical understanding of these issues.

III. SUMMARY AND DISCUSSION

We have studied the CDW quantum phase transition and its criticality in spinless fermions on a quasi-one-dimensional π-flux square lattice, by using iDMRG and bosonization. We find that the phase transition from a Dirac band insulator is continuous and its universality class is (1+1)D Ising with the central charge $c = 1/2$ when $L_y = 4n + 2 = 2, 6, \ldots$ under the periodic boundary condition, while that from a Dirac semimetal is Gaussian with $c = 2$ when $L_y = 4n = 4, 8, \ldots$. By introducing the twisted boundary condition, we discussed how the fermionic criticality of the Gaussian transition in the gapless Dirac semimetal is connected to the bosonic criticality of the Ising transition in the gapped Dirac band insulator. The global phase diagram was discussed, where the $c = 2$ critical point is connected to the $c = 1/2$ critical line. The resulting $c = 1/2$ critical line arises from the competition between the band mass and the density interaction leading to the CDW gap, and is described by the emergent Majorana fermions which are regarded as a fractionalized object. This could give insight for a comprehensive understanding of phase transitions in both metals and insulators. Our results could provide a basis to understand higher-dimensional systems, and also may be directly relevant for artificially created π-flux systems in cold atoms with a synthetic magnetic field [25,26].

Note added. Recently, we became aware of work which studies phase transitions between an anisotropic Dirac semimental and a band insulator [41].

ACKNOWLEDGMENTS

We are grateful to Y. Fuji for valuable discussions and constructive comments on our manuscript. We also thank J.-H. Chen, Y. Fukusumi, R. Kaneko, M. Nakamura, M. Oshikawa, B. Roy, S. Takayoshi, and Y. Yao for fruitful discussions. The numerical calculations have been done at Max Planck Institute for the Physics of Complex Systems. This work was supported by Grants-in-Aid for Scientific Research No. JP17K14333 and KAKENHI on Innovative Areas "J-Physics" (No. JP18H04318).

[1] T. Moriya and K. Ueda, Adv. Phys. **49**, 555 (2000).
[2] H. v. Löhneysen, A. Rosch, M. Vojta, and P. Wölfle, Rev. Mod. Phys. **79**, 1015 (2007).
[3] M. Brando, D. Belitz, F. M. Grosche, and T. R. Kirkpatrick, Rev. Mod. Phys. **88**, 025006 (2016).
[4] E. Berg, S. Lederer, Y. Schattner, and S. Trebst, Annu. Rev. Condens. Matter Phys. **10**, 63 (2019).
[5] T. Giamarchi, *Quantum Physics in One Dimension* (Oxford University Press, Oxford, UK, 2003).
[6] A. O. Gogolin, A. A. Nersesyan, and A. M. Tsvelik, *Bosonization and Strongly Correlated Systems* (Cambridge University Press, Cambridge, UK, 2004).
[7] S. Sorella and E. Tosatti, Europhys. Lett. **19**, 699 (1992).
[8] F. F. Assaad and I. F. Herbut, Phys. Rev. X **3**, 031010 (2013).
[9] L. Wang, P. Corboz, and M. Troyer, New J. Phys. **16**, 103008 (2014).
[10] L. Wang, Y.-H. Liu, and M. Troyer, Phys. Rev. B **93**, 155117 (2016).
[11] Z.-X. Li, Y.-F. Jiang, and H. Yao, Phys. Rev. B **91**, 241117(R) (2015).
[12] Z.-X. Li, Y.-F. Jiang, and H. Yao, New J. Phys. **17**, 085003 (2015).
[13] F. Parisen Toldin, M. Hohenadler, F. F. Assaad, and I. F. Herbut, Phys. Rev. B **91**, 165108 (2015).
[14] Y. Otsuka, S. Yunoki, and S. Sorella, Phys. Rev. X **6**, 011029 (2016).

[15] Z. Zhou, C. Wu, and Y. Wang, Phys. Rev. B **97**, 195122 (2018).
[16] P. Corboz, P. Czarnik, G. Kapteijns, and L. Tagliacozzo, Phys. Rev. X **8**, 031031 (2018).
[17] B. Rosenstein, H.-L. Yu, and A. Kovner, Phys. Lett. B **314**, 381 (1993).
[18] L. Rosa, P. Vitale, and C. Wetterich, Phys. Rev. Lett. **86**, 958 (2001).
[19] I. F. Herbut, Phys. Rev. Lett. **97**, 146401 (2006).
[20] I. F. Herbut, V. Juričić, and O. Vafek, Phys. Rev. B **80**, 075432 (2009).
[21] L. Janssen and I. F. Herbut, Phys. Rev. B **89**, 205403 (2014).
[22] B. Ihrig, L. N. Mihaila, and M. M. Scherer, Phys. Rev. B **98**, 125109 (2018).
[23] D.-H. Lee, Phys. Rev. Lett. **107**, 166806 (2011).
[24] M. Hohenadler, Z. Y. Meng, T. C. Lang, S. Wessel, A. Muramatsu, and F. F. Assaad, Phys. Rev. B **85**, 115132 (2012).
[25] J. Dalibard, F. Gerbier, G. Juzeliūnas, and P. Öhberg, Rev. Mod. Phys. **83**, 1523 (2011).
[26] T. Ozawa and H. M. Price, Nat. Rev. Phys. **1**, 349 (2019).
[27] S. R. White, Phys. Rev. Lett. **69**, 2863 (1992).
[28] U. Schollwöck, Rev. Mod. Phys. **77**, 259 (2005).
[29] U. Schollwöck, Ann. Phys. **326**, 96 (2011).
[30] I. P. McCulloch, arXiv:0804.2509.
[31] J. A. Kjäll, M. P. Zaletel, R. S. K. Mong, J. H. Bardarson, and F. Pollmann, Phys. Rev. B **87**, 235106 (2013).
[32] J. Hauschild and F. Pollmann, SciPost Phys. Lect. Notes, 5 (2018).
[33] P. Calabrese and J. Cardy, J. Stat. Mech.: Theory Exp. (2004) P06002.
[34] L. Balents and M. P. A. Fisher, Phys. Rev. B **55**, R11973 (1997).
[35] S. T. Carr, B. N. Narozhny, and A. A. Nersesyan, Phys. Rev. B **73**, 195114 (2006).
[36] Y.-C. He, M. P. Zaletel, M. Oshikawa, and F. Pollmann, Phys. Rev. X **7**, 031020 (2017).
[37] D. G. Shelton, A. A. Nersesyan, and A. M. Tsvelik, Phys. Rev. B **53**, 8521 (1996).
[38] D. G. Shelton and A. M. Tsvelik, Phys. Rev. B **53**, 14036 (1996).
[39] P. Lecheminant, A. O. Gogolin, and A. A. Nersesyan, Nucl. Phys. B **639**, 502 (2002).
[40] N. J. Robinson, A. Altland, R. Egger, N. M. Gergs, W. Li, D. Schuricht, A. M. Tsvelik, A. Weichselbaum, and R. M. Konik, Phys. Rev. Lett. **122**, 027201 (2019).
[41] B. Roy and M. S. Foster, Phys. Rev. X **8**, 011049 (2018).